Available online at www.sciencedirect.com
SCIENCE DIRECT®
Journal of Hydrology 281 (2003) 147–158
Journal of Hydrology
www.elsevier.com/locate/jhydrol

Hydraulics of horizontal wells in fractured shallow aquifer systems

Eungyu Park[a,*], Hongbin Zhan[b]

[a]Department of Civil Engineering and Geosciences, Delft University of Technology, P.O. Box 5028, Delft 2600GA, The Netherlands
[b]Department of Geology and Geophysics, Texas A&M University, College Station, TX 77843-3115, USA

Accepted 1 May 2003

Abstract

An analysis of groundwater hydraulic head in the vicinity of a horizontal well in fractured or porous aquifers considering confined, leaky confined, and water-table aquifer boundary conditions is presented. Solutions for hydraulic heads in both leaky confined and water table aquifers are provided. The fracture model used in this study is the standard double-porosity model. The aquitard storage is included in the formula. Solutions for the confined and unconfined conditions, fractured and porous conditions, wellbore storage, and skin effect are compared. Several findings of this study are, (1) the influence of wellbore storage and skin upon the drawdown for a fractured confined aquifer is similar to that for a porous confined aquifer, (2) aquitard storage affects the intermediate time the most by delaying the drawdown, and (3) there is a significant difference between the type curves of fractured and porous confined aquifers in most aquifer boundary conditions because of the contribution of matrix storage, and such a difference disappears at the later time.

Keywords: Horizontal well; Wellbore storage; Skin effect; Water table; Leaky confined aquifer; Fractured aquifer

1. Introduction

Horizontal well applications are one of the promising techniques in environmental remediation, water management, oil recovery, etc. In most of these applications, keeping the wellbore in contact with the targeting subsurface zone is essential. Horizontal wells offer many advantages over vertical wells because of their larger contact with the targeting aquifers.

There have been several studies about the hydraulics of horizontal wells in shallow ground water aquifers (Hantush and Papadopulos, 1962; Cleveland, 1994; Sawyer and Lieuallen-Dulam, 1998; Zhan et al., 2001) and in unsaturated zones (Falta, 1995; Zhan and Park, 2002). In most of these studies, the horizontal well is treated as a line sink/source and the wellbore storage and skin effects are not included. Zhan and Zlotnik (2002) derived solutions for drawdowns in water table aquifers due to pumping from horizontal and inclined wells. Their solutions may be inaccurate at early time and near the well because they neglect wellbore storage and skin effects. Recently, Park and Zhan (2002) derived a solution for hydraulic head in the vicinity of horizontal wells in confined and leaky confined

* Corresponding author. Present address: Environmental Science Division, Oak Ridge National Laboratory, Oak Ridge, TN, USA.
E-mail addresses: parke@ornl.gov (E. Park), zhan@hydrog.tamu.edu (H. Zhan).

0022-1694/03/$ - see front matter © 2003 Elsevier B.V. All rights reserved.
doi:10.1016/S0022-1694(03)00206-3

Nomenclature

A	area along outside of the horizontal wellbore (m^2)
C_w	conductance of wellbore skin (s^{-1})
d	thickness of the aquifer (m)
d_C	thickness of the aquitard (m)
d_{CD}	dimensionless d_c defined in Table 1
$\bar{f}_n$	function introduced in Eq. (A1)
$\bar{g}_0$	dimensionless point geometric function in Laplace domain
$\bar{g}^*$	dimensionless averaged geometric function of horizontal well in Laplace domain
h	hydraulic head (m)
$\bar{h}_D$	dimensionless h in Laplace domain
h'	hydraulic head in the matrix (m)
h_0	initial hydraulic head (m)
h_C	hydraulic head in the aquitard (m)
$K_0(u)$	second kind zero-order modified Bessel function
K_x, K_y, K_z	values of hydraulic conductivity in x-, y-, and z-directions, respectively (m/s)
K'	hydraulic conductivity of the matrix (m/s)
K_c	hydraulic conductivity of the aquitard (m/s)
L	screen length of horizontal wellbore (m)
L_D	dimensionless L defined in Table 1
p	Laplace transform variable with respect to dimensionless time
q_f	aquifer pumping rate for a point sink/source (m^3/s)
$\bar{q}_{fD}$	dimensionless q_f in Laplace domain
Q_f	total pumping rate (m^3/s)
$\bar{Q}_{fD}$	dimensionless total wellbore storage pumping rate in Laplace domain
r	variable in spherical coordinate (m)
r_D	dimensionless horizontal radial distance
r_m	radius of the matrix block (m)
r_{mD}	dimensionless r_m defined in Table 1
r_w	well radius (m)
r_{wD}	dimensionless r_w defined in Table 1
S_S	specific storage of the aquifer (m^{-1})
S_y	specific yield of the aquifer
S'_S	specific storage of the matrix (m^{-1})
S_{SC}	specific storage of the aquitard (m^{-1})
s	drawdown (m)
s_D	dimensionless drawdown defined in Table 1
$\bar{s}_D$	dimensionless drawdown in Laplace domain
s'	drawdown in matrix (m)
s_C	drawdown in aquitard (m)
t	time (s)
t_D	dimensionless time defined in Table 1
V	volume of finite diameter horizontal wellbore (m^3)
x, y, z	longitudinal, transversal, and vertical coordinates, respectively (m)
x_D, y_D, z_D	dimensionless x, y, and z, respectively
x_0, y_0, z_0	coordinates of the point source along x-, y-, and z-axis (m)
x_{0D}, y_{0D}, z_{0D}	dimensionless x_0, y_0, and z_0, respectively
z_w	depth from the central axis of the horizontal well to the lower boundary (m)
α	dimensionless skin conductance coefficient
α_1	empirical constant for water table drainage (s^{-1})
β	dimensionless wellbore storage coefficient
$\delta(u)$	Dirac delta function
ε_m	term introduced in Eq. (20) for a water table aquifer
Γ_1	inter-porosity flux between matrixes and fractures (s^{-1})
$\bar{\Gamma}_{1D}$	dimensionless Γ_1 in Laplace domain
Γ_2	leakage flux from adjacent aquifer (s^{-1})
$\bar{\Gamma}_{2D}$	dimensionless Γ_2 in Laplace domain
γ	dimensionless aquitard storage parameter defined in Table 1
η	dimensionless term introduced in Eq. (20) and defined in Table 1
θ	dimensionless term introduced in Eq. (20) and defined in Table 1
μ	dimensionless term introduced in Eq. (16) and defined in Table 1

σ	specific storage ratios between fracture and matrix	Ψ	dimensionless term introduced in Eq. (15)
ϕ	hydraulic conductivity ratio term defined in Table 1	ω	dimensionless term introduced in Eq. (16) and defined in Table 1

aquifers where the effects of wellbore storage and skin are included. However, their solution neglects the storage in the aquitard.

The double-porosity approach is used to simulate effects of a fractured aquifer on drawdown. This concept was introduced by Barenblatt et al. (1960). Later, it was applied by Warren and Root (1963) for a pseudo-steady state model, and by Kazemi (1969) for a transient model. The double-porosity concept is widely used to analyze hydraulic heads in the vicinity of vertical wells in fractured media; however only a few analytical studies (Ohaeri and Vo, 1991; Ozkan and Raghavan, 1991) of hydraulic head have used horizontal wells with the consideration of wellbore storage and skin effects, except in a few petroleum studies.

The objectives of this study include derivation of analytical solutions that consider effects caused by the finite diameter of a horizontal wellbore, and sensitivity analysis of various factors affecting the drawdown.

2. Mathematical model

2.1. Problem statement

The general configuration and the geometry of the problem for a fractured, water table aquifer can be seen in Fig. 1a, and for a fractured leaky aquifer in Fig. 1b. The origin of the coordinate system is at the lower boundary below the center of the horizontal wellbore, and the positive z-direction is upward. It is assumed that both aquifers have finite saturated thickness and infinite horizontal extent. The dashed lines in Fig. 1 are fractures and the cubic boxes there represent matrixes. Note that the simplified model of the fracture geometry, which has regular spacing and is perpendicular to the principal axes, is highly idealized in order to obtain closed-form solutions. Therefore the derived results based on this simple model can be used as a conceptual model only.

Because the depth range of the targeting aquifer system of this study is relatively shallow, the water-impeding skin material right outside the matrix block is not considered in this study (e.g. Moench, 1984). The aquifer and the fluid are slightly compressible and have constant physical properties. We assume that the horizontal well has a finite-diameter and a finite screen length. The central axis of the well is along the x-axis from $-L/2$ to $L/2$, where L is the screen length of the horizontal wellbore, and the cross section of the horizontal well is a circular area with the diameter of $2r_w$ (Park and Zhan, 2002). The depth from the central axis of the horizontal well to the lower boundary is z_w. The governing equation of hydraulic head in the vicinity of a point sink/source in a three-dimensionally anisotropic fractured aquifer (Dougherty and Babu, 1984),

$$K_x\frac{\partial^2 h}{\partial x^2}+K_y\frac{\partial^2 h}{\partial y^2}+K_z\frac{\partial^2 h}{\partial z^2}-\Gamma_1-\Gamma_2-S_S\frac{\partial h}{\partial t}=q_f(t)\delta(x-x_0)\delta(y-y_0)\delta(z-z_0), \quad (1)$$

where K_x, K_y, K_z is hydraulic conductivity (m/s) in the x-, y-, and z-directions of the fractures, respectively; h is hydraulic head (m); S_S is specific storage (m^{-1}); t is time (s); q_f is the aquifer pumping rate for a point sink/source (m^3/s) ($q_f > 0$ corresponds to pumping); $\delta(u)$ is the Dirac delta function; (x_0, y_0, z_0) is the point source location; Γ_1 is the fracture-matrix water exchange term, or the surface inter-porosity flux term (1/s) (Deruyck et al., 1982); and Γ_2 is the inter-aquifer flux (leakage) term (1/s). If $\Gamma_1 \to 0$, Eq. (1) reduces to the governing equation of a single-porosity aquifer; and if $\Gamma_2 \to 0$, Eq. (1) reduces to the governing equation of a confined aquifer.

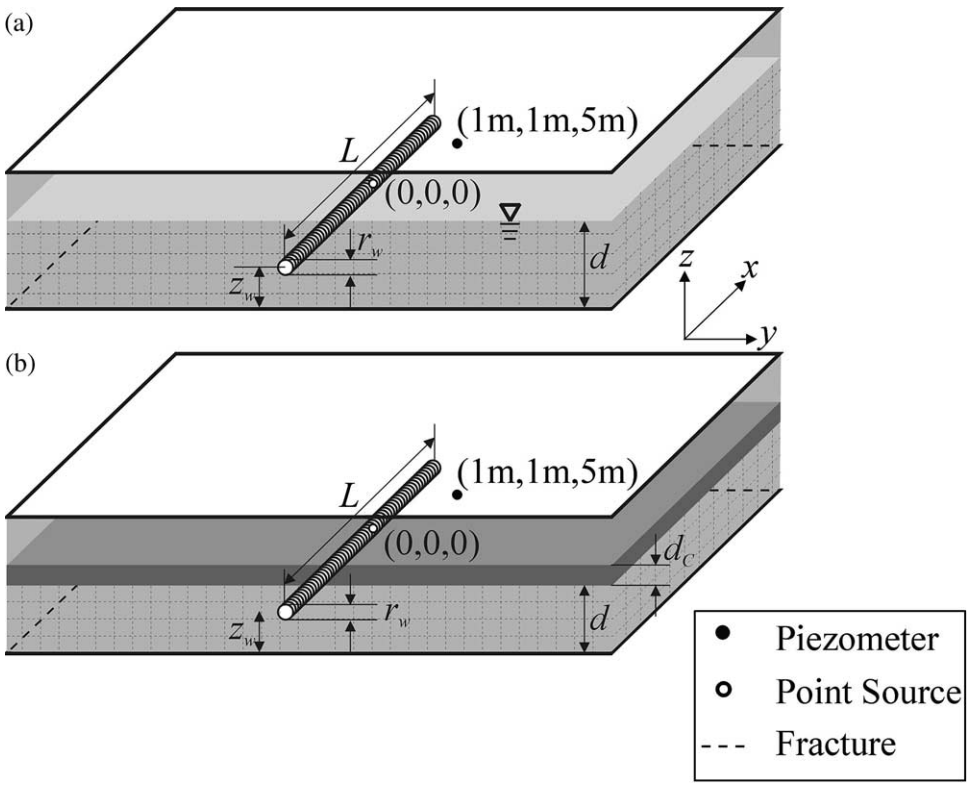

Fig. 1. Schematic diagrams of a finite-diameter horizontal well in (a) a fractured water-table aquifer, and (b) a fractured leaky confined aquifer.

The problem-solving process is divided into two parts. First, the point source solution is derived. Following Park and Zhan (2002), the finite volume horizontal wellbore can be represented as superposition of point sources, and the pumping rate, Q_f, can be defined as

$$Q_f(t) = \frac{1}{V}\int_V q_f(x,y,z,t)\mathrm{d}V, \tag{2}$$

where V is the volume of the horizontal wellbore and $q_f(x,y,z,t)/V$ is the point source strength. To apply the above equation, an infinitely large value of hydraulic conductivity is assumed within the wellbore volume.

The boundary conditions in the horizontal plane at infinity are

$$h(x,y,z,t)|_{x=\pm\infty} = h_0, \quad h(x,y,z,t)|_{y=\pm\infty} = h_0, \tag{3}$$

where h_0 is the initial head (m). The condition at the lower no-flow boundary is

$$\partial h(x,y,z,t)/\partial z|_{z=0} = 0, \tag{4}$$

and at the upper boundary for a leaky confined aquifer is (see Fig. 1b)

$$\partial h(x,y,z,t)/\partial z|_{z=d} = 0, \tag{5}$$

by assuming the leaky confining layer as an internal source of water uniformly distributed inside the aquifer, where d is the aquifer thickness (m).

In this study we apply the delayed drainage model for a water table boundary (Boulton, 1963; Moench, 1997),

$$K_z\,\partial h(x,y,d,t)/\partial z = -\alpha_1 S_y \int_0^t \partial h(x,y,d,t)/\partial\tau \times \exp\{-\alpha_1(t-\tau)\}\mathrm{d}\tau, \tag{6}$$

where α_1 is an empirical constant and S_y is the specific yield.

The initial condition is

$$h(x,y,z,t)|_{t=0} = h_0. \tag{7}$$

A double-porosity approach is used to model the flux (Γ_1) between the matrixes and fractures, and the subsidiary equation for a spherically approximated matrix block is (Deruyck et al., 1982)

$$\frac{K'}{r^2}\frac{\partial}{\partial r}\left(r^2\frac{\partial h'}{\partial r}\right) = S'_S\frac{\partial h'}{\partial t}, \tag{8}$$

where K' is the hydraulic conductivity (m/s), S'_S is the specific storage (m^{-1}), and h' is the hydraulic head (m), all referring to the matrix. The inter-porosity flux is (Deruyck et al., 1982)

$$\Gamma_1 = \frac{3K'}{r_m}\left(\frac{\partial h'}{\partial r}\right)\Big|_{r=r_m}, \tag{9}$$

where r_m is the radius (m) of the matrix block.

The initial and boundary conditions for matrixes are, respectively

$$h'|_{t=0} = h_0 \qquad \text{and } h'|_{r=r_m} = h. \tag{10}$$

The inter-aquifer flux (leakage) term is given by Γ_2. Where the aquifer is confined by an aquitard, only the vertical flux is considered in the aquitard and the governing equation is (Hantush, 1960)

$$K_C\frac{\partial^2 h_C}{\partial z^2} = S_{SC}\frac{\partial h_C}{\partial t}, \tag{11}$$

where K_C is the hydraulic conductivity (m/s), h_C is the hydraulic head (m), and S_{SC} is the specific storage, all referring to the aquitard (m^{-1}). It follows that the inter-aquifer flux is given by

$$\Gamma_2 = \frac{K_C}{d}\frac{\partial h_C}{\partial z}\Big|_{z=d_C}, \tag{12}$$

where d_C is the thickness of the aquitard (m). The initial upper and lower boundary conditions for the aquitard are

$$h_C|_{t=0} = h_0, \quad h_C|_{z=0} = h_0 \quad \text{and } h_C|_{z=d_C} = h. \tag{13}$$

The head, h, is changed to drawdown, $s = h_0 - h$. The dimensionless parameters are defined in Table 1 and all the parameters are identified in the Notation. The variables for the subsidiary equations (Eqs. (8) and (11)), h' and h_C are also changed into $s' = h_0 - h'$ and $s_C = h_0 - h_C$, respectively, and converted into dimensionless parameters.

Table 1
Dimensionless parameters

$s_D = \frac{4\pi\sqrt{K_xK_y}d}{q}s$	$\beta = \frac{4\sqrt{K_xK_y}S_Sd^3}{K_zr_c^2}$
$x_D = \frac{x}{d}\sqrt{\frac{K_z}{K_x}}$, $y_D = \frac{y}{d}\sqrt{\frac{K_z}{K_y}}$, $z_D = \frac{z}{d}$	$\phi = \frac{K_C}{K_z}$
$t_D = \frac{K_z}{S_Sd^2}t$	$\theta = \frac{S_Sd}{S_y}$
$\Gamma_{1D} = \frac{4\pi d^3\sqrt{K_xK_y}}{qK_z}\Gamma_1$, $\Gamma_{2D} = \frac{4\pi d^3\sqrt{K_xK_y}}{qK_C}\Gamma_2$	$\gamma = \frac{S_{SC}K_z}{S_SK_C}$
$L_D = \frac{L}{d}\sqrt{\frac{K_z}{K_x}}$	$\mu = \frac{3K'}{r_{mD}K_z}$
$r_D = \frac{r}{d}$, $r_{mD} = \frac{r}{d}$, $r_{wD} = \frac{r}{d}$	$\omega = \frac{K'S_S}{K_zS'_S}$
$d_{CD} = \frac{d_C}{d}$	$\sigma = \frac{S'_S}{S_S}$
$\alpha = \frac{r_wLC_S}{2d\sqrt{K_xK_y}}$	$\eta = \frac{\alpha_1S_yd}{K_z}$

2.2. Solution in the Laplace domain

By introducing the dimensionless variables (Table 1) and applying a Laplace transformation with respect to time, we obtain the equation from Eq. (1) as

$$\frac{\partial^2\bar{s}_D}{\partial x_D^2} + \frac{\partial^2\bar{s}_D}{\partial y_D^2} + \frac{\partial^2\bar{s}_D}{\partial z_D^2} - \bar{\Gamma}_{1D} - \bar{\Gamma}_{2D} - p\bar{s}_D = \frac{4\pi\bar{q}_{fD}(p)\delta(x_D - x_{0D})\delta(y_D - y_{0D})\delta(z_D - z_{0D})}{p}, \tag{14}$$

where bar denotes a term in the Laplace domain and the subscript D refers to a dimensionless term defined

in Table 1. The parameters used in the following solutions are explained in the nomenclature. Solving Eq. (14) (Hantush, 1960; Deruyck et al., 1982) gives

$$\nabla^2 \bar{s}_D - \Psi^2 \bar{s}_D = \frac{4\pi \bar{q}_{fD}(p)\delta(x_D - x_{0D})\delta(y_D - y_{0D})\delta(z_D - z_{0D})}{p} \tag{15}$$

where

$$\Psi = \sqrt{\phi\sqrt{\gamma p}\coth(d_{CD}\sqrt{\gamma p}) + \mu\left\{\sqrt{\frac{p}{\omega}}\coth\left(\sqrt{\frac{p}{\omega}}r_{mD}\right) - \frac{1}{r_{mD}}\right\} + p}, \tag{16}$$

The first term inside the square root sign is related to the leakage through the aquitard, and the second term is related to the flow between the matrixes and the fractures.

Eqs. (3)–(7) become, after introduction of dimensionless parameters (Table 1) and Laplace transformations,

$$\bar{s}_D(x_D, y_D, z_D, p)|_{x_D=\pm\infty} = 0, \qquad \bar{s}_D(x_D, y_D, z_D, p)|_{y_D=\pm\infty} = 0, \tag{17}$$

and

$$\partial \bar{s}_D(x_D, y_D, z_D, p)/\partial z_D|_{z_D=0} = 0. \tag{18}$$

The upper boundary condition can be either a no-flow boundary

$$\partial \bar{s}_D(x_D, y_D, z_D, p)/\partial z_D|_{z_D=1} = 0, \tag{19}$$

or a free boundary (water-table aquifer) (Moench, 1997)

$$\frac{\partial \bar{s}_D(x_D, y_D, 1, p)}{\partial z_D} = -\eta \frac{p\bar{s}_D(x_D, y_D, 1, p)}{p + \eta\theta}. \tag{20}$$

The solutions for Eq. (15) subject to conditions (17)–(20) are (details in Appendix A)

$$\bar{s}_D(x_D, y_D, z_D, p) = \frac{\bar{Q}_{fD}}{V}\int_v \bar{g}_0\, dV = \frac{\bar{Q}_{fD}}{V}\int_v \left[2K_0(r_D\Psi) + 4\sum_{n=1}^{\infty}\cos(n\pi z_D)\cos(n\pi z_{0D})K_0(r_D\sqrt{\Psi^2 + n^2\pi^2})\right] dV, \tag{21}$$

for a leaky confined aquifer, and

$$\bar{s}_D(x_D, y_D, z_D, p) = \frac{\bar{Q}_{fD}}{V}\int_v \sum_{n=1}^{\infty}\frac{4\cos(\varepsilon_m z_D)\cos(\varepsilon_m z_{0D})}{1 + 0.5\sin(2\varepsilon_m)/\varepsilon_m} \times K_0(r_D\sqrt{\Psi^2 + \varepsilon_m^2})dV, \tag{22}$$

for a water table aquifer, where

$$\varepsilon_m \tan(\varepsilon_m) = \frac{\eta p}{p + \eta\theta},\ m = 0, 1, 2, \ldots$$

2.3. Aquifer pumping rate

Wellbore storage can affect the early time or the near field hydraulic heads. In most applications, long wellbores are used to lengthen the contact with the aquifer. The pumping rate measured at a monitoring piezometer outside of the wellbore for a finite-diameter horizontal wellbore in the Laplace domain, $\bar{Q}_{fD}$, is (Park and Zhan, 2002)

$$\bar{Q}_{fD}(p) = \frac{\alpha\beta}{p[p\{1 + \alpha\bar{g}^*(p)\} + \alpha\beta]}, \tag{23}$$

where α and β are defined in Table 1, $\bar{g}^*$ is the surface average of the geometric functions (Park and Zhan, 2002) and is related to the average hydraulic head outside the well skin. The pumping rate measured inside the wellbore where the flux to the wellbore is assumed to be uniform (Park and Zhan, 2002) is

$$\bar{Q}_{fD} = \frac{\beta\{1 + \bar{g}^*(p)\}}{p[p\{1 + \alpha\bar{g}^*(p)\} + \alpha\beta]}. \tag{24}$$

The skin is assumed to be infinitesimally thin when using Eqs. (23)–(24). This treatment is similar to that of Dougherty and Babu (1984) and Kabala and Cassiani (1997), and others in studying vertical wells.

In this study, the surface average of the geometric function, $\bar{g}^*$, is (Park and Zhan, 2002)

$$\bar{g}^*(p) = \frac{1}{VA}\int_A\int_V \bar{g}_0(x_D, y_D, z_D; x_{0D}, y_{0D}, z_{0D}, p)dV\, dA, \tag{25}$$

where V is the volume of the horizontal wellbore, A is the area right outside of the wellbore, and $\bar{g}_0$ is

the point geometric function which was previously defined by Park and Zhan (2002).

For most of the horizontal well applications, the lengths of the wellbores are long and the wellbore storages and skin effects can be important at early time (Park and Zhan, 2002). Under these conditions, Eq. (25) can be approximated by employing several identities used in previous studies (Hantush, 1964; Zhan et al., 2001). For confined and leaky confined aquifers, the surface average of the geometric function can be approximated as

$$\bar{g}^*(p) \approx \frac{2\pi}{L_D}\left\{\frac{1}{\sqrt{p+\Psi^2}} + 2\sum_{n=1}^{\infty}\cos^2(n\pi z_{wD}) \times \frac{1}{\sqrt{p+\Psi^2+n^2\pi^2}}\right\}, \quad (26)$$

and for water table aquifers, it is

$$\bar{g}^*(p) \approx \frac{4\pi\cos(\varepsilon_m z_{0D})^2}{L_D\{1+0.5\sin(2\varepsilon_m)/\varepsilon_m\}\sqrt{p+\Psi^2+\varepsilon_m^2}}. \quad (27)$$

The derivation of Eqs. (26) and (27) follows the same procedure presented by Park and Zhan (2002).

2.4. Software

For most of the practical calculations, the geometric function of a finite diameter horizontal wellbore can be simplified by reducing the dimensions of the integration. Park and Zhan (2002) pointed out that the finite-diameter geometric function is computationally demanding, but that its effect only exists during very early time and converges to the line geometric function as $t_D/(x_D^2+y_D^2) \rightarrow 0.01$ in an isotropic aquifer if the wellbore storage is excluded. Therefore, the finite-diameter geometric function can be approximately substituted by the line geometric function mostly since early time. The inverse Laplace transform will result in the solution in real-time domain (Stehfest, 1970; de Hoog et al, 1982; Hollenbeck, 1998). The MATLAB script used for this study, FINHOW2, is available from the author's website: http://geoweb.tamu.edu/Faculty/Zhan/Research.html.

This program can handle six types of aquifer conditions: confined, leaky confined, and water table aquifers, and each of them can be either fractured or porous. It uses up to 21 controllable hydrogeologic parameters: d, d_c, K_x, K_y, K_z, K', K_c, r_m, S_S, S_y, S'_S, S_{SC}, α_1, and well parameters C_w, L, r_w, Q, x, y, z, z_w (see nomenclature).

3. Sensitivity analyses

We perform several sensitivity analyses on the aquifer conditions (i.e. confined, leaky confined, and water-table aquifers), the aquifer properties (i.e. specific storage of the aquitard, hydraulic conductivity of the matrix, and specific storage of the matrix), and the well properties (i.e. wellbore storage and skin effects) using the derived solutions and the default parameter values that are presented in Table 2. One should keep in mind that basic conclusions are limited to a range of parameters that are considered in our analyses. The hypothetical piezometer of all

Table 2
Hypothetical default parameters used for sensitivity analyses

Parameter	Default value
D	10 m
K_x, K_y, K_z	0.0001 m/s (isotropic if not specified)
S_S	0.00002 m^{-1}
Q	0.001 m^3/s
L	100 m
z_w	5 m
r_w	0.1 m
C_S	0.0001 s^{-1}
Fractured aquifer	
K'	0.00001 m/s (if not specified)
S'_S	0.001 m^{-1} (if not specified)
r_m	1 m
Leaky aquifer	
K_C	0.000001 m/s
S_{SC}	0.0001 m^{-1}
d_C	1 m
Water-table aquifer	
S_y	0.2
α_1	100 m/s
Monitoring piezometer	
(x, y, z)	(1 m, 1 m, 5 m)

following analyses is located at (1, 1, and 5 m) in the x, y, and z- coordinate system (Fig. 1).

3.1. Comparison between confined and water-table aquifers

We compare the drawdown patterns of fractured or porous, confined and water-table aquifers in early, intermediate, and later time using derived solutions. The hypothetical responses of the aquifer systems are presented in Fig. 2. Note that the drawdown in a fractured aquifer always refers to the effects in the fractures, not in the matrix. As expected, horizontal well pumping in a water-table aquifer causes much less drawdown than that in a confined aquifer, especially after the intermediate time when the water is supplied by the gravity drainage. In a confined aquifer that is either fractured or porous, there is a difference between a fractured aquifer and a porous aquifer in later time drawdown history. That is because water is extracted from storage in a confined aquifer; a fractured confined aquifer has extra storage water from the matrix in additional to the fractures, and thus should have less drawdown than a porous confined aquifer. In a water-table aquifer, the drawdown for both fractured and porous cases converges at the later time and almost no effect of matrix flow occurs. The reason for this is that after the intermediate time, the gravity drainage supplies water to the aquifer. Such relatively superior water storage substantially surpasses any difference of storage water contributions from a fractured and porous aquifer. Therefore, the difference between fractured and porous water-table aquifers caused by the matrix flow at early time disappears at the later time.

3.2. Wellbore storage and skin effects

To verify the wellbore storage effects, analyses of dimensionless radii of horizontal wellbores of 0.001, 0.01, 0.02, 0.03, and 0.1 were compared with a given skin conductance of 0.0001 s^{-1} in a fractured confined aquifer and a fractured water table aquifer (Fig. 3). The wellbore storage effects in both fractured confined aquifers and fractured water table aquifer are similar to those in porous confined aquifers (Park and Zhan, 2002): a larger dimensionless wellbore radius has greater and longer lasting wellbore storage effect.

In regard to the skin effect, the results of fractured confined aquifers and fractured water table aquifers are also similar to those in porous confined aquifers

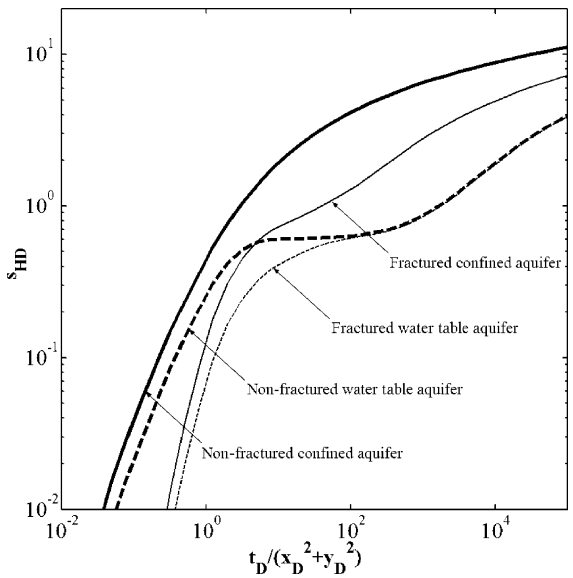

Fig. 2. Dimensionless drawdown versus dimensionless times for different aquifer types and media.

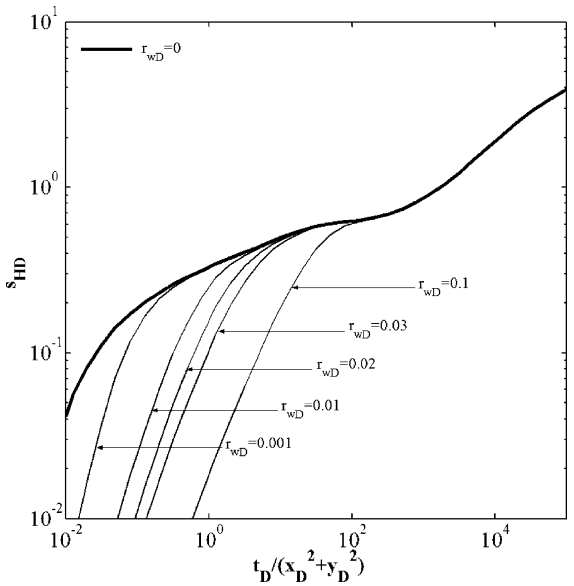

Fig. 3. Dimensionless drawdown of different wellbore radii in a fractured water-table aquifer.

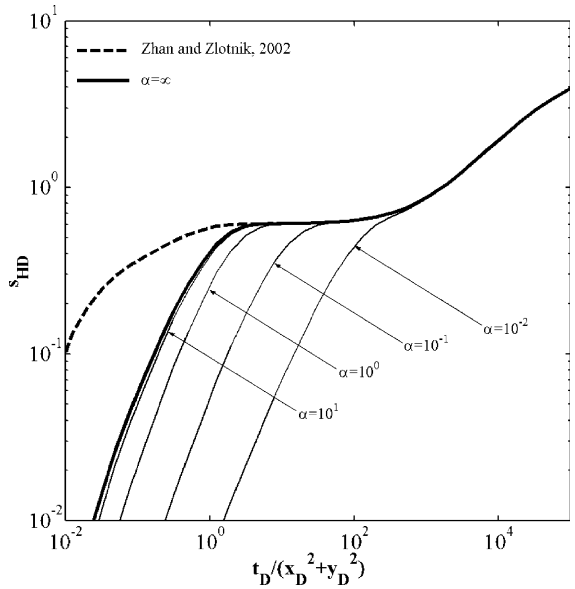

Fig. 4. Dimensionless drawdown of different skin parameters (α) in a porous water-table aquifer. Ideal response (wellbore storage and no skin) of the aquifer (bold line) and the previous study (bold dash line) is compared with several different dimensionless skin parameters ($\alpha = 0.01$, 0.1, 1, and 10).

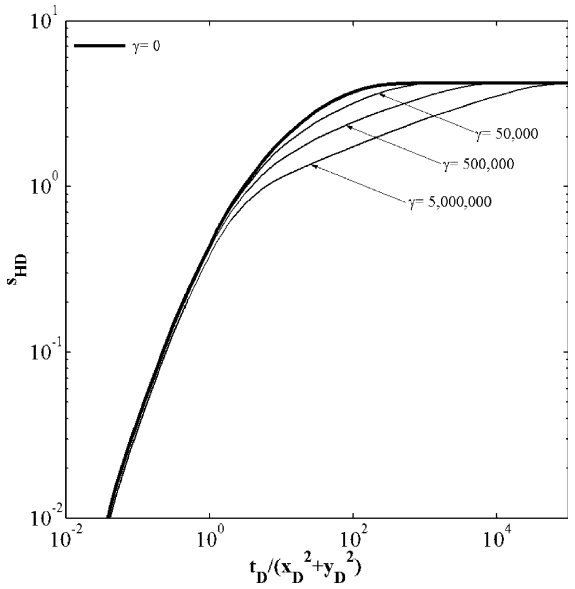

Fig. 5. Dimensionless drawdown of drawdown for different aquitard storage parameters ($\gamma = 50,000$, 500,000, and 5,000,000).

(Park and Zhan, 2002). Fig. 4 compares the dimensionless drawdown patterns of four different skin effects ($\alpha = 0.01$, 0.1, 1, and 10). We also compare our solution with that of an infinitesimal well radius without skin in a water table aquifer (Zhan and Zlotnik, 2002). The type curves converge at the later time. Furthermore, the smaller the α, the longer it takes to converge. For instance, for $\alpha = 10^0$ and 10^{-2}, the type curves converge to the type curve of Zhan and Zlotnik (2002) at approximately at $t_D/(x_D^2 + y_D^2) = 10$ and 10^3, respectively. Using the default parameters (Table 1), these correspond to $t = 4$ and 400 s, respectively. This indicates that after the first several minutes of pumping, the Zhan and Zlotnik (2002) model can be used for many practical applications.

3.3. Specific storage of the aquitard

A sensitivity analysis was performed on the dimensionless aquitard storage parameter (γ), which is proportional to the aquitard specific storage. If the aquitard storage is important (silt/clay), the water supply from the aquitard storage supplies water to the aquifer and depresses the drawdown of the aquifer during the intermediate time when compared to the case without the aquitard storage ($\gamma = 0$) (Fig. 5). The highest value of dimensionless aquitard storage parameters shows the greatest deviation from the negligible aquitard storage model by depressing the drawdown curve during intermediate time. It is interesting to note that at the later time, the storage water from the aquitard is depleted and all type curves merge with the type curve for the case of $\gamma = 0$.

3.4. Hydraulic conductivity of the matrix

Several matrix/fracture hydraulic conductivity ratios (K'/K_z) of 10^{-1}, 10^{-3}, 10^{-5}, and 10^{-7} under $\sigma = 50$ were tested for a confined aquifer (Fig. 6). The result (Fig. 6) shows that the higher value of matrix hydraulic conductivity (higher K'/K_z value) results in a lower drawdown at a given time. Moreover, the type curves with different K'/K_z values merge to a common curve at late times, and the smaller the K'/K_z value, the longer time it takes to merge with common curve. The type curves with different K'/K_z values depart from the type curve for porous media developed by Park and Zhan (2002), and the larger the K'/K_z value, the earlier it starts to depart.

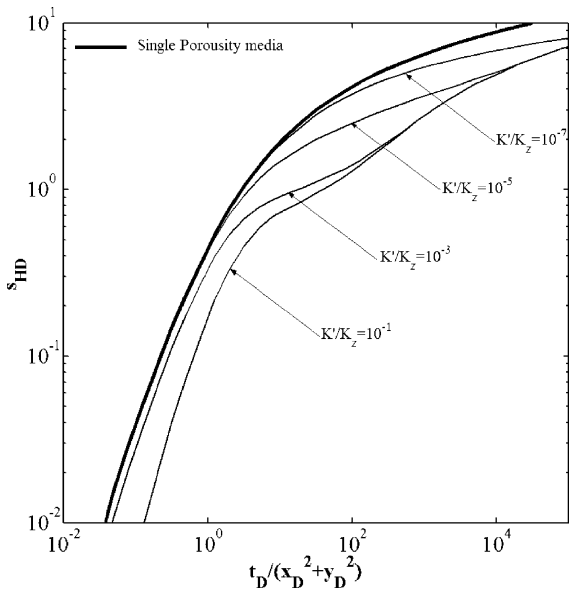

Fig. 6. Effects of different hydraulic conductivity values ($K'/K_z = 10^{-1}$, 10^{-3}, 10^{-5}, and 10^{-7}) of the matrix in fractured confined aquifers.

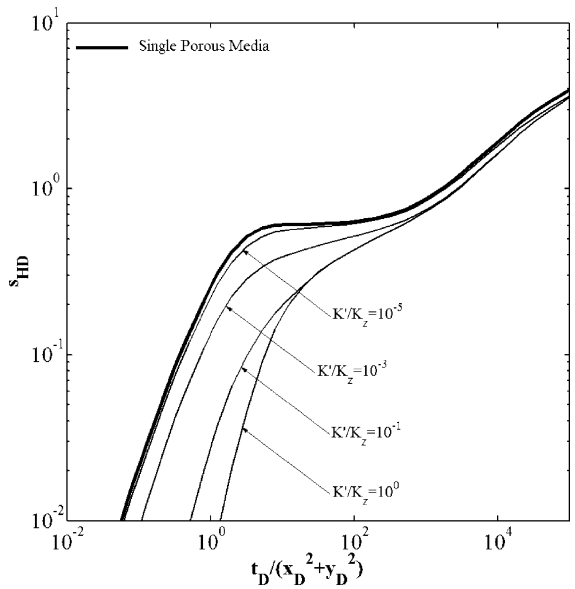

Fig. 7. Effects of different hydraulic conductivity values ($K'/K_z = 10^{0}$, 10^{-1}, 10^{-3}, and 10^{-5}) of the matrix in fractured water-table aquifers.

The same matrix/fracture hydraulic conductivity ratios (K'/K_z) of 10^{-1}, 10^{-3}, 10^{-5}, and 10^{-7} under $\sigma = 50$ were applied to a water-table aquifer (Fig. 7). The masking early response of the aquifer and their masking periods are similar to that of a fractured confined aquifer. Fig. 7 shows that one can apply the porous aquifer solution to the fractured system in a water-table aquifer if the contrast of the hydraulic conductivity between the fracture and the matrix is very large ($K'/K_z \leq 10^{-5}$). According to this analysis, one generally cannot ignore the water flow from the matrix to the fracture even if the hydraulic conductivity of the matrix is small compared with that of fracture.

3.5. Specific storage of the matrix

Ratios between specific storage of fracture and matrix (σ) of 5000, 500, 50, and 5 under $K'/K_z = 10^{-5}$ were tested (Fig. 8). Drawdown curves follow the single porosity at early times and then depart from the curve of a single porosity case. The depart times depend on σ. An analysis shows that when the specific storage of the matrix is small, the fractured aquifer solution converges to the porous aquifer solution. However, in many cases, the matrix systems have much higher storage properties than fracture systems, thus the fractured aquifer solutions may be substantially different from the porous aquifer

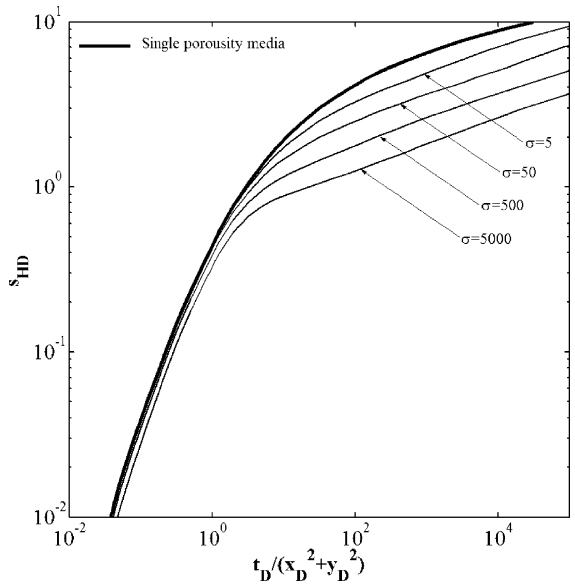

Fig. 8. Effects of different specific storage values ($\sigma = 5$, 50, 500, and 5000) of the matrix in fractured confined aquifers.

solutions. In contrast, in a fractured water-table aquifer system, the solution is much less sensitive to σ because the drawdown depends more on the water from the water table drainage than from the storage.

4. Conclusions

Three-dimensional semi-analytical solutions for finite-diameter horizontal wells in fractured shallow aquifer systems, i.e. water-table aquifers and leaky confined aquifers, were derived. The derived solutions expand previous finite-diameter well solutions by considering fractured media and including the aquitard storage (Park and Zhan, 2002). In addition, the solutions generalize previous horizontal well solutions for water-table aquifers by including wellbore storage and skin effects (Zhan and Zlotnik, 2002).

A graphically integrated numerical MATLAB program named FINHOW2 is developed to facilitate the input and output handling. This program can handle various aquifer conditions described by as many as 21 aquifer and well parameters.

For relatively general conditions, drawdown is more sensitive to the hydraulic conductivity and storage of the matrix in a fractured confined aquifer than in a fractured water table aquifer. There is an appreciable difference between a fractured aquifer and a porous aquifer at late time by supplying water from matrixes to fractures after intermediate time. In a water-table aquifer, the drawdown for both fractured and porous cases converge at late time.

The wellbore storage effects in both fractured confined aquifers and fractured water table aquifer are similar to those in porous conditions (Park and Zhan, 2002). This finding indicates that the wellbore storage effect substantially surpasses the matrix-fracture flow effect at the early pumping stage in a fractured aquifer. In regard to the skin effect, the results of fractured confined aquifers and fractured water table aquifers are also similar to those in porous conditions (Park and Zhan, 2002). For practical purposes, the skin effect is usually negligible after the first several minutes of pumping in a water table aquifer. In a case where the aquitard storage is non-negligible (silt/clay), the water supply from the aquitard storage plays a role during the intermediate time when compared to the case without the aquitard storage.

Several interesting results are found with different matrix/fracture hydraulic conductivity ratios (K'/K_z) in a confined aquifer. The type curves with different K'/K_z values depart from the type curve for a single porosity aquifer. The porous aquifer solution can be applied to the fractured aquifer system in a water-table aquifer if the contrast of the hydraulic conductivity between the fracture and the matrix is large ($K'/K_z \leq 10^{-5}$). Generally, the water flow from the matrix to the fracture cannot be ignored even if the hydraulic conductivity of the matrix is small compared to that of the fracture.

In a fractured confined aquifer, the solution is sensitive to the specific storage ratio; but in a fractured water table aquifer, the solution is less sensitive to the specific storage ratio.

Acknowledgements

Support for this work was provided by the US National Science Foundation Grant No. BES-9909964, the Geological Society of America Grant No. 6980-01, and by the Office of the Vice President for Research and Associate Provost for Graduate Studies at Texas A&M University through the Interdisciplinary Research Initiatives. We thank Dr V.A. Zlotnik, Dr L. Murdoch, and Dr H.M. Haitjema for their detailed and very constructive comments on this manuscript.

Appendix A

Eq. (15) subject to boundary conditions in Eqs. (17)–(20) follows previous studies (Dougherty and Babu, 1984; Moench, 1997; Zhan et al., 2001; Park and Zhan, 2002). The proposed solution is

$$\bar{s}_{\mathrm{D}}(x_{\mathrm{D}},y_{\mathrm{D}},z_{\mathrm{D}},p)=\sum_{n=0}^{\infty}\bar{f}_n(x_{\mathrm{D}},y_{\mathrm{D}};x_{0\mathrm{D}},y_{0\mathrm{D}},p)\cos(\varepsilon_n z_{\mathrm{D}}), \tag{A1}$$

where $\bar{s}_{\mathrm{D}}$ is the dimensionless drawdown in the Laplace domain, $\bar{f}_n$ is a function that depends on the horizontal coordinate and p, and ε_n is a spatial frequency term. The boundary conditions, Eqs. (17)–(19), are satisfied using the solution procedure after Park and Zhan (2002) (p. 399). Using Eqs. (17), (18)

and (20), by applying Eq. (A1) to Eq. (20), one obtains equation for ε_m

$$\varepsilon_n \tan(\varepsilon_n) = \frac{\eta p}{p + \eta\theta}, \ m = 0, 1, 2, \ldots \tag{A2}$$

By applying Eq. (A1) into Eq. (15), multiplying $\cos(\varepsilon_m z_{0D})$, and integrating from the lower boundary ($z_D = 0$) to the upper boundary ($z_D = 1$) along z-axis, one obtains

$$\begin{aligned}(\Psi^2 + \varepsilon_n^2)\bar{f}_D &= \frac{\partial^2 \bar{f}_D}{\partial x_D^2} + \frac{\partial^2 \bar{f}_D}{\partial y_D^2} \\ &\quad + \frac{8\pi \bar{q}_{fD}(p)\delta(x_D - x_{0D})\delta(y_D - y_{0D})\cos(\varepsilon_n z_{0D})}{1 + 0.5\sin(2\varepsilon_n)/\varepsilon_n}.\end{aligned} \tag{A3}$$

The solution for Eq. (A3) is

$$\begin{aligned}&\bar{f}_D(x_D, y_D, z_D; x_{0D}, y_{0D}, z_{0D}, p) \\ &= \sum_{m=0}^{\infty} \frac{4\cos(\varepsilon_n z_{0D})\cos(\varepsilon_n z_D)}{1 + 0.5\sin(2\varepsilon_n)/\varepsilon_n} K_0(r_D\sqrt{\Psi^2 + \varepsilon_n^2}),\end{aligned} \tag{A4}$$

where $r_D = [(x_D - x_{0D})^2 + (y_D - y_{0D})^2]^{1/2}$ is the dimensionless horizontal radial distance between the source point, (x_{0D}, y_{0D}, z_{0D}), and the measuring point, (x_D, y_D, z_D), and $K_0(x)$ is the second kind, zero order, modified Bessel function.

References

Barenblatt, G.I., Zheltov, I.P., Kocina, I.N., 1960. Basic concepts in the theory of seepage of homogeneous liquids in fissured rocks. J. Appl. Math. Mech. Engl. Transl. 24, 1286–1303.

Boulton, N.S., 1963. Analysis of data from non-equilibrium pumping tests allowing for delayed yield from storage. Proc. Inst. Civil Eng. 26, 469–482.

Cleveland, T.G., 1994. Recovery performance for vertical and horizontal wells using semianalytical simulation. Ground Water 32 (1), 103–107.

Deruyck, B.G., Bourdet, D.P., DaPrat, G., Ramey, H.J. Jr., 1982. Interpretation of interference tests in reservoirs with double porosity behavior, Theory and field examples, SPE Paper 11025, Society of Petroleum Engineering of AIME, Dallas, TX.

Dougherty, D.E., Babu, D.K., 1984. Flow to a partially penetrating well in a double-porosity reservoir. Water Resour. Res. 20 (8), 1116–1122.

Falta, R.W., 1995. Analytical solutions for gas flow due to gas injection and extraction from horizontal wells. Ground Water 33 (2), 235–246.

Hantush, M.S., 1960. Modification of the theory of leaky aquifers. J. Geophys. Res. 65 (11), 3713–3716.

Hantush, M.S., Papadopulos, I.S., 1962. Flow of ground water to collector wells. J. Hydraul. Div., Proc. Am. Soc. Civil Engrs HY 5, 221–244.

Hantush, M.S., 1964. Hydraulics of wells. In: Chow, V.T. (Ed.). Advances in Hydroscience. Academic Press, New York.

Hollenbeck, K.J., 1998. INVLAP.M, A MATLAB function for numerical inversion of Laplace transforms by the de Hoog algorithm, http://www.isva.dtu.dk/staff/karl/invlap.htm

de Hoog, F.R., Knight, J.H., Stokes, A.N., 1982. An improved method for numerical inversion of Laplace transforms. SIAM J. Sci. Stat. Comp. 3, 357–366.

Kabala, Z.J., Cassiani, G., 1997. Well hydraulics with the Weber–Goldstein transforms. Transport in Porous Media 29 (2), 225–246.

Kazemi, H., 1969. Pressure Transient Analysis of Naturally Fractured Reservoirs, Trans. AIME, 256, 451–461.

Moench, A.F., 1984. Double-porosity models for a fissured groundwater reservoir with fracture skin. Water Resour. Res. 20 (7), 831–846.

Moench, A.F., 1997. Flow to a well of finite diameter in a homogeneous, anisotropic water table aquifer. Water Resour. Res. 33 (6), 1397–1407.

Ohaeri, C.U., Vo, D.T., 1991. Practical solutions for interactive horizontal well test analysis, SPE Paper 22729, Society of Petroleum Engineering of AIME, Dallas, TX.

Ozkan, E., Raghavan, R., 1991. New solutions for well-test-analysis problems, Part 1—analytical considerations. SPE Formation Eval. September, 359–368.

Park, E., Zhan, H., 2002. Hydraulics of a finite diameter horizontal well with wellbore storage and skin effect in leaky aquifers. Adv. Water Resour. 25 (4), 389–400.

Sawyer, C.S., Lieuallen-Dulam, K.K., 1998. Productivity comparison of horizontal and vertical ground water remediation well scenarios. Ground Water 36 (1), 98–103.

Stehfest, H., 1970. Numerical inversion of Laplace transforms. Commun. ACM 13 (1), 47–49.

Warren, J.E., Root, R.J., 1963. The behavior of naturally fractured reservoirs. Trans. Am. Inst. Min. Metall. Pet. Eng. 228, 245–255.

Zhan, H., Park, E., 2002. Vapor flow to horizontal wells in vadose zones. Soil Sci. Soc. Am. J. 66 (3), 710–721.

Zhan, H., Zlotnik, V.A., 2002. Groundwater flow to horizontal and slanted wells in unconfined aquifers. Water Resour. Res. 38 (7), 13.1–13.11.

Zhan, H., Wang, L.V., Park, E., 2001. On the horizontal-well pumping tests in anisotropic confined aquifers. J. Hydrol. 252 (1–4), 37–50.